

## **DIFFRACTION BY DIELECTRIC-LOADED MULTIPLE SLITS IN A CONDUCTING PLANE: TM CASE**

**D.-J. Lee<sup>\*</sup>, S.-J. Lee, W.-S. Lee, and J.-W. Yu**

Department of Electrical Engineering, KAIST, 291 Daehak-ro, Yuseong-gu, Daejeon 305-701, Korea

**Abstract**—A new and exact series solution for the scattering and coupling problems by dielectric-loaded multiple slits in a perfectly conducting screen is presented. The case of normal incidence and TM polarization is considered. The scattered and transmitted fields are represented in terms of an infinite series of radial modes. By applying the appropriate boundary conditions, the coefficients of scattered and transmitted fields are obtained and some numerical results are given.

### **1. INTRODUCTION**

The diffraction of electromagnetic radiation by slits has been widely studied for microwave and optical applications [1–3]. The problem of a single slit has been treated by several researchers using different methods [4–6]. A method of moments analysis of electromagnetic coupling through a single slot and multiple slots was formulated using either the characteristic-mode theory [7, 8] or a Gaussian-beam expansion [9]. A method of moments solution for the problem of a single slot and for a double slot was also treated by Otsuki [10], using Babinet's principle. Diffraction by a single slit, by double slits, and by multiple slits was investigated by a method that uses a set of orthogonal functions and Fourier transformations [11–13]. When the slit (or strip grating) is infinite, there is an enormous amount of theoretical work before, its scattering behavior can be well understood [14–19]. When the strip grating is finite, the problem also receives much attention. When the strip grating is loaded by dielectric material and finite, the amount of relevant theoretical works seems very small, and its

---

*Received 13 August 2012, Accepted 3 September 2012, Scheduled 17 September 2012*

\* Corresponding author: Dong-Jin Lee (dong905@kaist.ac.kr).

scattering behavior is not well understood. In this paper we limit our discussion to scattering from the dielectric-loaded finite strip grating. The understanding of transmission through the dielectric-loaded finite strip grating is important in the evaluation and control of aperture leakage often encountered in antenna and electromagnetic interference (EMI) problems. Also, a diffraction problem from dielectric-loaded multiple slits is not only an interesting subject in the field of electromagnetic wave theory but also an important one relating to the surface measurement or diagnostics by microwave, millimeter wave, laser or ultrasonic beams, and specially to the development of various kinds of optical devices. The purpose of the present paper is to study scattering from a dielectric-loaded finite strip grating (i.e., dielectric-loaded multiple slits) by using radial mode matching technique [20].

## 2. THEORETICAL FORMULATION

Consider a  $TM_z$  plane wave incident on a perfectly conducting plane with dielectric-loaded  $N$ -slits as shown in Fig. 1. The direction of the incident field makes an angle  $\phi_i$  with the  $x$  axis. Regions (I), (II) and (III) denote the upper, inner, and lower sections of dielectric cylinder, respectively. The radius of each cylinder is  $a_r$  ( $r = 1, 2, \dots, N$ ). Throughout the paper,  $e^{j\omega t}$  time harmonic factor is suppressed. In region (I) ( $\rho_r > a_r$ ,  $0 < \phi < \pi$ ,  $r = 1, 2, \dots, N$ ) as shown in Fig. 1, the incident, reflected and scattered electric fields of  $l$ th cylinder are given by [21]

$$E_{zl}^{inc}(\rho_l, \phi_l) + E_{zl}^{ref}(\rho_l, \phi_l) = \sum_{p=1}^{\infty} s_p^l J_p(k_o \rho_l) \sin p\phi_l \quad (1)$$

$$E_{zl}^{scat}(\rho_l, \phi_l) = \sum_{p=1}^{\infty} B_p^l H_p^{(2)}(k_o \rho_l) \sin p\phi_l \quad (2)$$

where  $s_p^l = 4j^p e^{jk_o x_l \cos \phi_i} \sin p\phi_i$ ,  $k_o = w\sqrt{\mu_o \varepsilon_o}$  and  $B_p^l$  are referred to as the scattering coefficients of  $l$ th cylinder.  $J_p(\cdot)$  and  $H_p^{(2)}(\cdot)$  are the  $p$ th order Bessel function of the first kind and Hankel function of the second kind, respectively. The incident wave is chosen to have a phase of zero at the origin, so that  $k_o x_l \cos \phi_i$  is the phase of the incident wave at the center of  $l$ th cylinder. The total fields in region (I) should include the original incident, reflected fields and the scattered fields from cylinders  $1, 2, \dots, N$ , respectively and it can be expressed by the

following forms: when  $r = l$ ,

$$\begin{aligned} E_{zl}^I(\rho_l, \phi_l) &= E_{zl}^{inc}(\rho_l, \phi_l) + E_{zl}^{ref}(\rho_l, \phi_l) + \sum_{r=1}^N E_{zr}^{scat}(\rho_r, \phi_r) \\ &= \sum_{p=1}^{\infty} \left\{ s_p^l J_p(k_o \rho_l) \sin p \phi_l + \sum_{r=1}^N B_p^r H_p^{(2)}(k_o \rho_r) \sin p \phi_r \right\} \quad (3) \end{aligned}$$

Since  $H_\phi = 1/(jw\mu_0)\partial E_z(\rho, \phi)/\partial \rho$ , the corresponding  $\phi$  component of the  $H$ -field in region (I) is

$$H_{\phi l}^I(\rho_l, \phi_l) = \frac{k_o}{jw\mu_0} \sum_{p=1}^{\infty} \left\{ s_p^l J_p'(k_o \rho_l) \sin p \phi_l + \sum_{r=1}^N B_p^r H_p^{(2)'}(k_o \rho_r) \sin p \phi_r \right\} \quad (4)$$

and  $\mu_0$  is a background medium of permeability in all regions.

The  $z$ -component of the transmitted electric field in region (III) ( $\rho_r > a_r$ ,  $\pi < \phi < 2\pi$ ) from the  $l$ th slit can be written as

$$E_{zl}^{III}(\rho_l, \phi_l) = \sum_{p=1}^{\infty} C_p^l H_p^{(2)}(k_o \rho_l) \sin p(\phi_l - \pi) \quad (5)$$

The corresponding magnetic field in region (III) from the  $l$ th slit is

$$H_{\phi l}^{III}(\rho_l, \phi_l) = \frac{k_o}{jw\mu_0} \sum_{p=1}^{\infty} C_p^l H_p^{(2)'}(k_o \rho_l) \sin p(\phi_l - \pi) \quad (6)$$

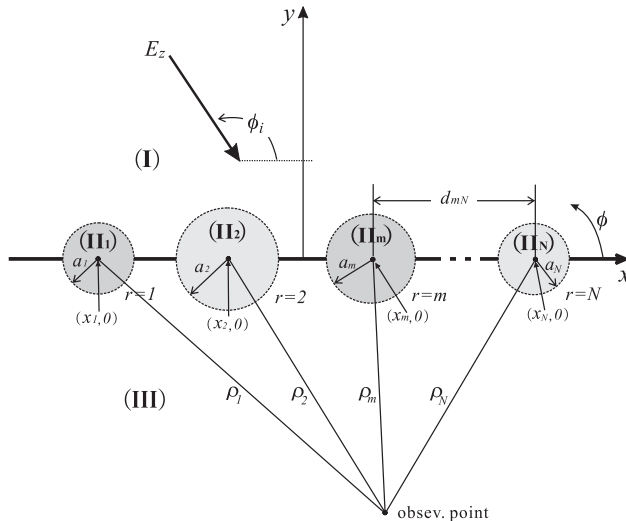


Figure 1. Geometry of the problem.

Similarly, the  $z$ -component of the electric field inside cylinder  $l$  can be written as

$$E_{zl}^{II}(\rho_l, \phi_l) = \sum_{n=-\infty}^{\infty} A_n^l J_n(k_l \rho_l) e^{jn\phi_l} \quad (7)$$

where  $k_l = k_o \sqrt{\varepsilon_l / \varepsilon_0}$ . To determine the unknown coefficients  $A_n^l$ ,  $B_p^l$  and  $C_p^l$  ( $l = 1, 2, 3, \dots, N$ ), it is necessary to match the boundary conditions of tangential  $E$ - and  $H$ -field continuities at  $\rho_l = a_l$ . To apply boundary conditions at  $\rho_l = a_l$ , the fields outside the cylinder  $l$  must be expressed in terms of the coordinate of the cylinder  $l$ . In other words,  $(\rho_r, \phi_r)$  in Eq. (3) and the corresponding equation obtained from Eq. (5) must be transformed to  $(\rho_l, \phi_l)$ . This is possible using the addition theorem for cylindrical Bessel and Hankel functions [22]. Therefore these equations can be written as

$$E_{zl}^I(\rho_l, \phi_l) = \sum_{p=1}^{\infty} \left\{ s_p^l J_p(k_o \rho_l) \sin p\phi_l + B_p^l H_p^{(2)}(k_o \rho_l) \sin p\phi_l \right. \\ \left. + \sum_{r=1, r \neq l}^N \sum_{m=-\infty}^{\infty} B_p^r W_{pm}^{lr}(k_o \rho_l) \sin m\phi_l \right\} \quad (8)$$

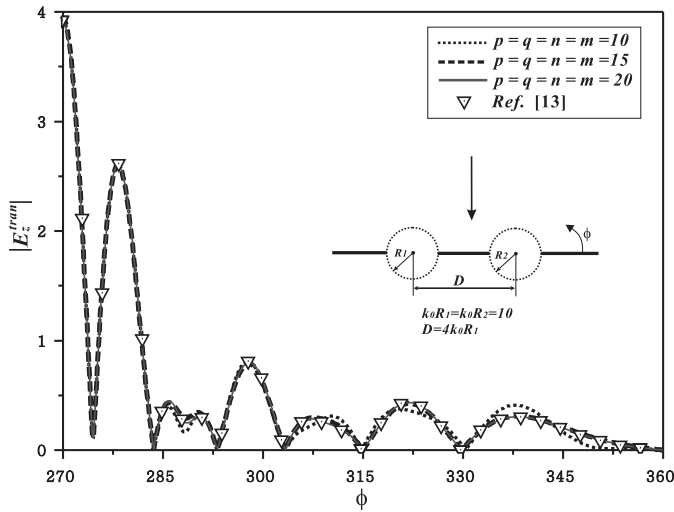


**Figure 2.** Far-zone transmitted field  $|E_z^{\text{tran}}|$  ( $\epsilon_1 = \epsilon_2 = 1.0$ ,  $k_0 R_1 = k_0 R_2 = 10$ ,  $D = 4k_0 R_1$ ,  $\phi_i = 90^\circ$ ).

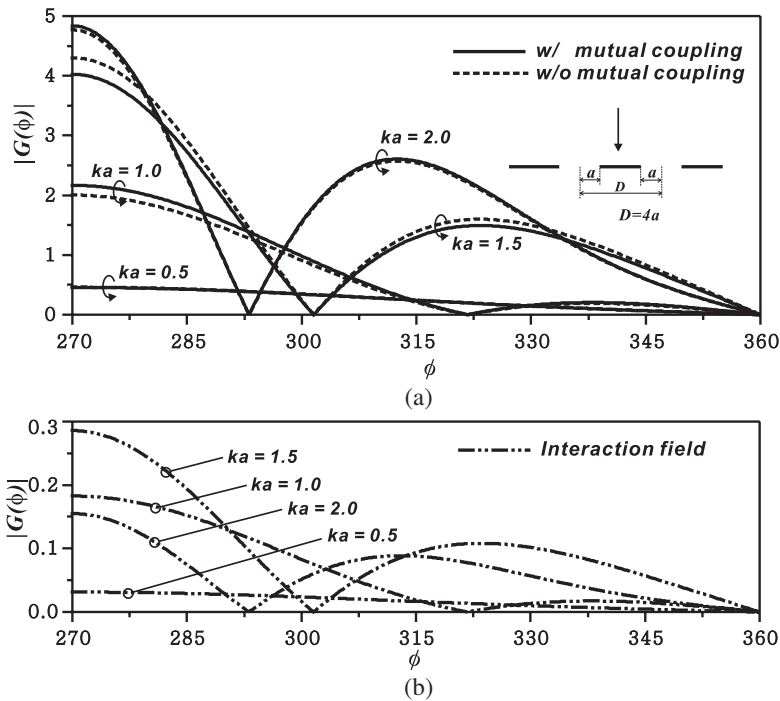


**Figure 3.** Transmitted field pattern ( $|G(\phi)|$ ) from two identical slits with  $ka = 0.5, 1.0, 1.5, 2.0$  at  $\phi_i = 90^\circ$ .

$$E_{zl}^{III}(\rho_l, \phi_l) = \sum_{p=1}^{\infty} \left\{ C_p^l H_p^{(2)}(k_o \rho_l) \sin p(\phi_l - \pi) \right. \\ \left. + \sum_{r=1, r \neq l}^N \sum_{m=-\infty}^{\infty} C_p^r W_{pm}^{lr}(k_o \rho_l) \sin m(\phi_l - \pi) \right\} \quad (9)$$

where

$$W_{pm}^{lr}(k_o \rho_l) = \begin{cases} -(-1)^p H_{p+m}^{(2)}(k_0 d_{lr}) J_m(k_0 \rho_l), & r > l \\ -(-1)^m H_{p+m}^{(2)}(k_0 d_{lr}) J_m(k_0 \rho_l), & r < l \end{cases} \quad (10)$$

in which  $d_{lr}$  is the distance between cylinders  $l$  and  $r$ . The tangential electric field continuity at  $\rho_l = a_l$  yields

$$E_{zl}^{II} = \begin{cases} E_z^I, & \rho_l = a_l, 0 < \phi < \pi \\ E_z^{III}, & \rho_l = a_l, \pi < \phi < 2\pi \end{cases} \quad (11)$$

Substituting Eqs. (7), (8) and (9) into (11) gives

$$\begin{aligned}
 & \sum_{p=1}^{\infty} \left\{ s_p^l J_p(k_o a_l) \sin p \phi_l + B_p^l H_p^{(2)}(k_o a_l) \sin p \phi_l \right. \\
 & + \sum_{r=1, r \neq l}^N \sum_{m=-\infty}^{\infty} B_p^r W_{pm}^{lr}(k_o a_l) \sin m \phi_l \left. \right\} U_I \\
 & + \sum_{p=1}^{\infty} \left\{ C_p^l H_p^{(2)}(k_o a_l) \sin p(\phi_l - \pi) \right. \\
 & + \sum_{r=1, r \neq l}^N \sum_{m=-\infty}^{\infty} C_p^r W_{pm}^{lr}(k_o a_l) \sin m(\phi_l - \pi) \left. \right\} U_{II} = \sum_{n=-\infty}^{\infty} A_n^l J_n(k_l a_l) e^{jn \phi_l} \quad (12)
 \end{aligned}$$

where  $U_{I(II)} = 1$  for  $0 < \phi < \pi$  ( $\pi < \phi < 2\pi$ ) and zero elsewhere. In Eq. (12), applying the orthogonality condition of exponential function

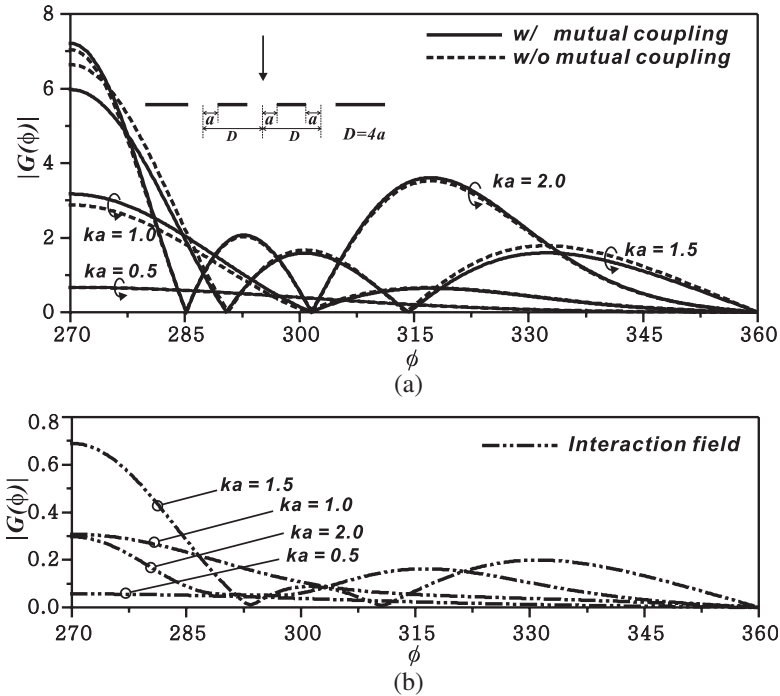


**Figure 4.** Transmitted field pattern ( $|G(\phi)|$ ) from three identical slits with  $ka = 0.5, 1.0, 1.5, 2.0$  at  $\phi_i = 90^\circ$ .

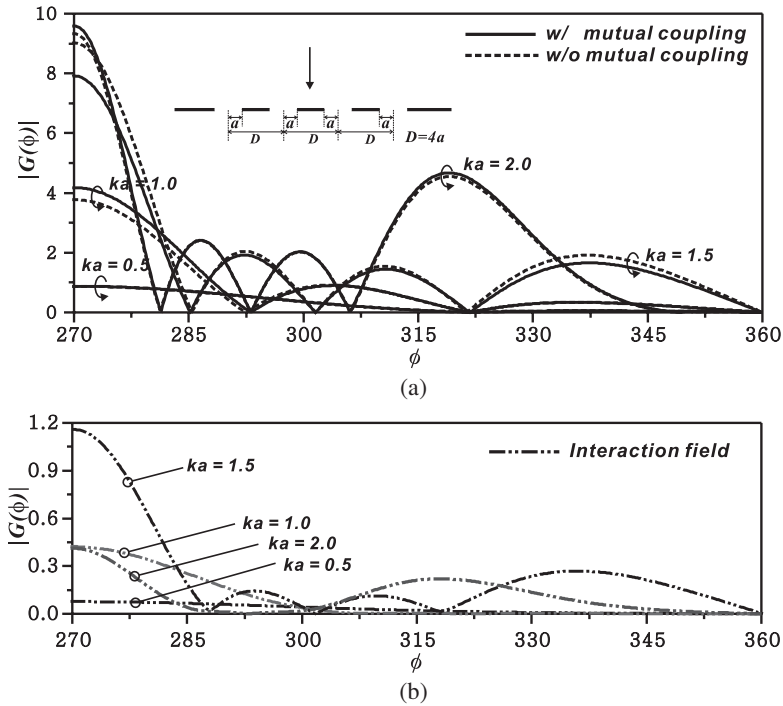


**Figure 5.** Transmitted field pattern ( $|G(\phi)|$ ) from four identical slits with  $ka = 0.5, 1.0, 1.5, 2.0$  at  $\phi_i = 90^\circ$ .

with respect to  $\phi$  from 0 to  $2\pi$  gives

$$\begin{aligned}
 2\pi A_k^l J_k(k_l a_l) &= \sum_{p=1}^{\infty} \left\{ s_p^l J_p(k_o a_l) + B_p^l H_p^{(2)}(k_o a_l) \right\} F_{-kp}^l \\
 &+ \sum_{p=1}^{\infty} \sum_{r=1, r \neq l}^N \sum_{m=-\infty}^{\infty} B_p^r W_{pm}^{lr}(k_o a_l) F_{-km}^l + \sum_{p=1}^{\infty} C_p^l H_p^{(2)}(k_o a_l) G_{-kp}^l \\
 &+ \sum_{p=1}^{\infty} \sum_{r=1, r \neq l}^N \sum_{m=-\infty}^{\infty} C_p^r W_{pm}^{lr}(k_o a_l) G_{-km}^l
 \end{aligned} \quad (13)$$

where

$$F_{-kp}^l = \int_0^\pi e^{-jk\phi_l} \sin p\phi_l d\phi_l \quad (14)$$

$$G_{-kp}^l = \int_\pi^{2\pi} e^{-jk\phi_l} \sin p(\phi_l - \pi) d\phi_l \quad (15)$$

Next, the tangential magnetic field continuities at  $\rho_l = a_l$  yield

$$H_{\phi_l}^{II_l} = H_{\phi_l}^I, \quad 0 < \phi_l < \pi \quad (16)$$

$$H_{\phi_l}^{II_l} = H_{\phi_l}^{III}, \quad \pi < \phi_l < 2\pi \quad (17)$$

Since,  $H_\phi(\rho, \phi) = k/(jw\mu_0)\partial E_z(\rho, \phi)/\partial(k\rho)$ , the  $H_\phi$  continuities at  $\rho_l = a_l$  are given by

$$\begin{aligned} & \sum_{p=1}^{\infty} s_p^l J_p'(k_o a_l) \sin p\phi_l + \sum_{p=1}^{\infty} B_p^l H_p^{(2)'}(k_o a_l) \sin p\phi_l \\ & + \sum_{p=1}^{\infty} \sum_{r=1, r \neq l}^N \sum_{m=-\infty}^{\infty} B_p^r W_{pm}^{l'r}(k_o a_l) \sin m\phi_l \\ & = \frac{k_l}{k_o} \sum_{n=-\infty}^{\infty} A_n^l J_n'(k_l a_l) e^{jn\phi_l}, \quad 0 < \phi_l < \pi \end{aligned} \quad (18)$$

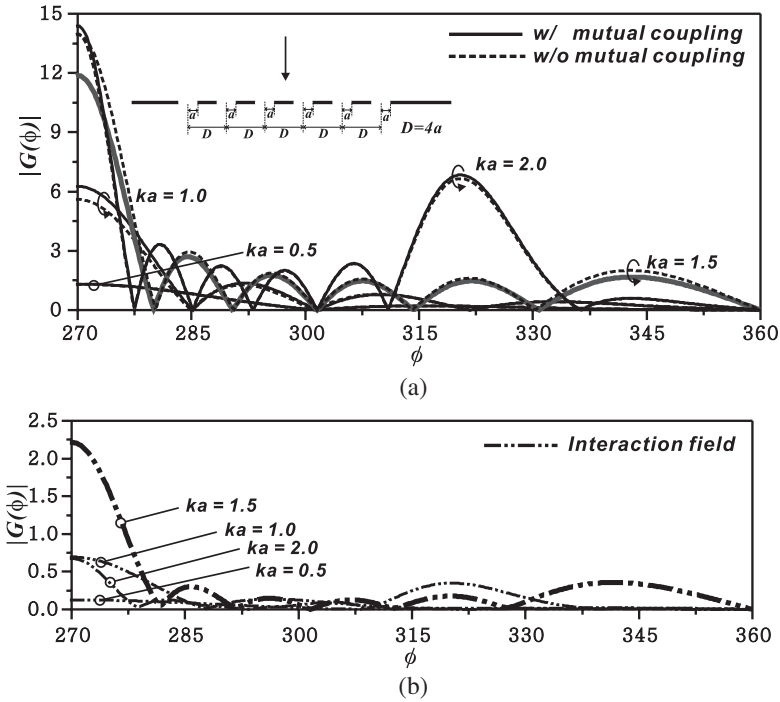


**Figure 6.** Transmitted field pattern ( $|G(\phi)|$ ) from six identical slits versus  $ka = 0.5, 1.0, 1.5, 2.0$  at  $\phi_i = 90^\circ$ .



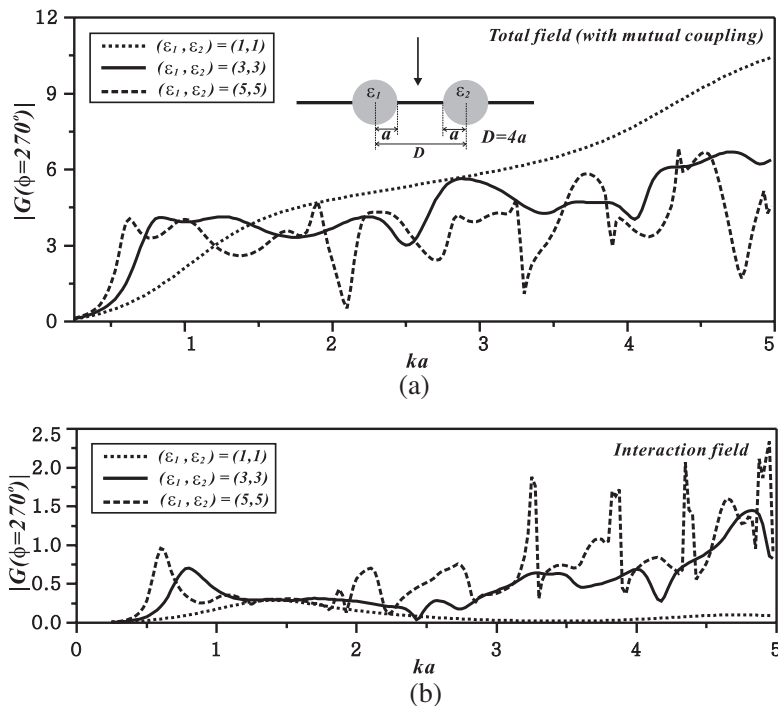


**Figure 7.** Transmitted field pattern ( $|G(\phi = 270^\circ)|$ ) from four identical slits versus  $ka$  at  $\phi_i = 90^\circ$ .

$$\begin{aligned}
 & \sum_{p=1}^{\infty} C_p^l H_p^{(2)'}(k_o a_l) \sin p(\phi_l - \pi) \\
 & + \sum_{p=1}^{\infty} \sum_{r=1, r \neq l}^N \sum_{m=-\infty}^{\infty} C_p^r W_{pm}^{l r}(k_o a_l) \sin m(\phi_l - \pi) \\
 & = \frac{k_l}{k_o} \sum_{n=-\infty}^{\infty} A_n^l J_n'(k_l a_l) e^{j n \phi_l}, \quad \pi < \phi_l < 2\pi
 \end{aligned} \quad (19)$$

In a similar manner, applying orthogonality conditions of sine function to Eqs. (18) and (19) with respect to  $\phi_l$  from 0 to  $\pi$  and from  $\pi$  to  $2\pi$  yield

$$\begin{aligned}
& s_q^l J_q'^l(k_o a_l) + B_q^l H_q^{(2)'}(k_o a_l) + \sum_{p=1}^{\infty} \sum_{r=1, r \neq l}^N B_p^r \left\{ W_{qp}^{l'r}(k_o a_l) - W_{(-q)p}^{l'r}(k_o a_l) \right\} \\
& = \frac{2}{\pi} \frac{k_l}{k_o} \sum_{n=-\infty}^{\infty} A_n^l J_n'(k_l a_l) F_{qn}^l
\end{aligned} \tag{20}$$

$$\begin{aligned}
& C_q^l H_q^{(2)'}(k_o a_l) + \sum_{p=1}^{\infty} \sum_{r=1, r \neq l}^N C_p^r \left\{ W_{qp}^{l'r}(k_o a_l) - W_{(-q)p}^{l'r}(k_o a_l) \right\} \\
& = \frac{2}{\pi} \frac{k_l}{k_o} \sum_{n=-\infty}^{\infty} A_n^l J_n'(k_l a_l) G_{qn}^l
\end{aligned} \tag{21}$$

Substituting Eq. (13) into (20) and (21), the simultaneous system equations for unknown coefficients  $B_p^l$  and  $C_p^l$  ( $l = 1, 2, 3, \dots, N$ ) are

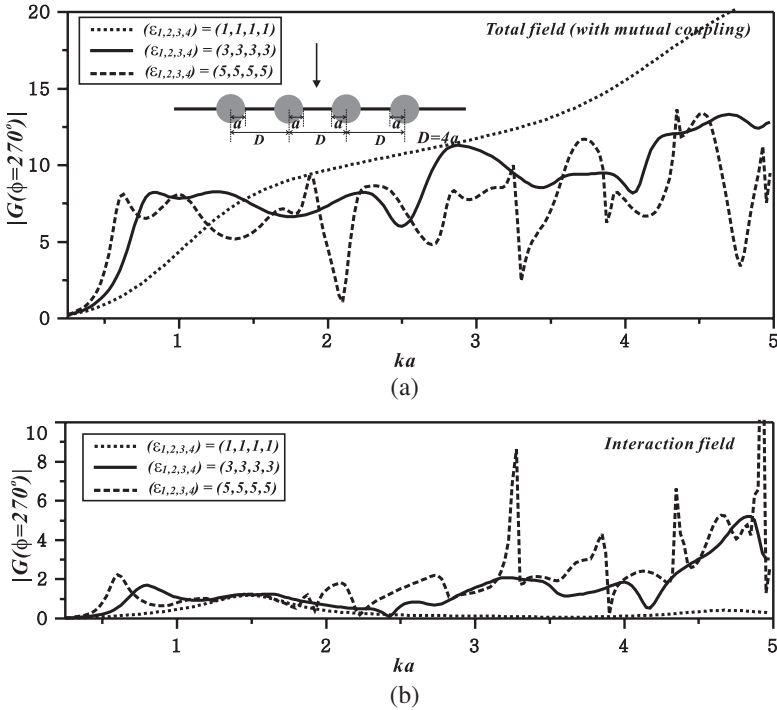


**Figure 8.** Transmitted field pattern ( $|G(\phi)| = 270^\circ$ ) from four identical slits versus  $ka = 1.5$  at  $\phi_i = 90^\circ$ .

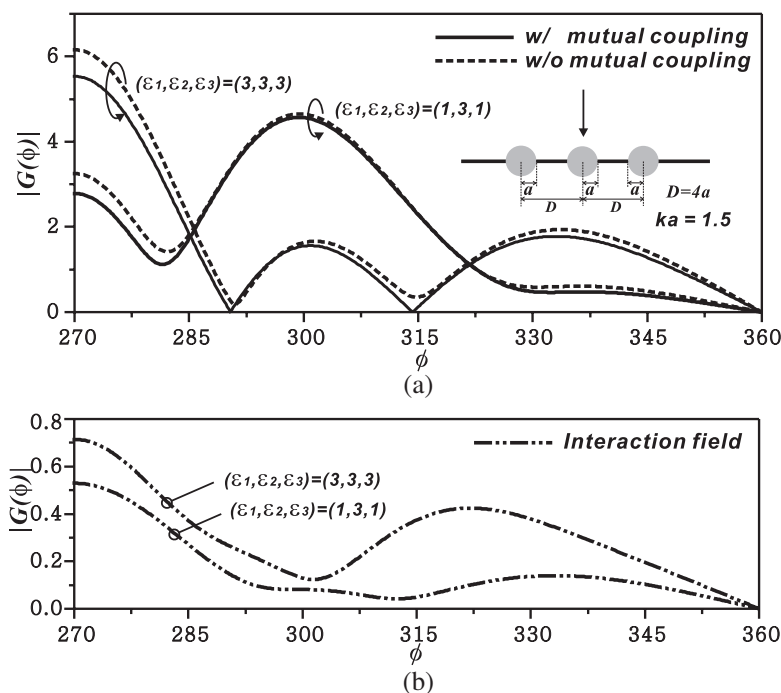


**Figure 9.** Transmitted field pattern ( $|G(\phi)|$ ) from dielectric-loaded four slits with  $ka = 1.5$  at  $\phi_i = 90^\circ$ .

given by

$$\begin{bmatrix} \alpha_q^1 \\ \beta_q^1 \\ \vdots \\ \alpha_q^N \\ \beta_q^N \end{bmatrix} = \begin{bmatrix} [S_{11}^{11}] & [S_{12}^{11}] \\ [S_{21}^{11}] & [S_{22}^{11}] \\ \vdots & \vdots \\ [S_{11}^{N1}] & [S_{12}^{N1}] \\ [S_{21}^{N1}] & [S_{22}^{N1}] \end{bmatrix} \cdots \begin{bmatrix} [S_{11}^{1N}] & [S_{12}^{1N}] \\ [S_{21}^{1N}] & [S_{22}^{1N}] \\ \vdots & \vdots \\ [S_{11}^{NN}] & [S_{12}^{NN}] \\ [S_{21}^{NN}] & [S_{22}^{NN}] \end{bmatrix} \begin{bmatrix} B_p^1 \\ C_p^1 \\ \vdots \\ B_p^N \\ C_p^N \end{bmatrix} \quad (22)$$

The submatrices  $[S_{ij}^{lr}]$  are given by

$$[S_{ij}^{lr}] = \begin{cases} [c_{qp}^{lr}], & l = r \quad (\text{self-interaction}) \\ [d_{qp}^{lr}], & l \neq r \quad (\text{mutual-interaction}) \end{cases} \quad (23)$$

and the elements  $c_{qp}^{lr}$  and  $d_{qp}^{lr}$  are given by

$$\begin{bmatrix} c_{qp}^{lr} \end{bmatrix} = H_p^{(2)'}(k_o a_l) \delta_{qp} \delta_{ij} - H_p^{(2)}(k_o a_l) I_{ij}^l \quad (24)$$

$$\begin{bmatrix} d_{qp}^{lr} \end{bmatrix} = \left( W_{pq}^{lr} - W_{p(-q)}^{lr} \right) \delta_{ij} - R_{ij}^{lr} \quad (25)$$

where

$$I_{ij}^l = \frac{k_l}{\pi^2 k_o} \sum_{n=-\infty}^{\infty} \frac{J_n'(k_l a_l)}{J_n(k_l a_l)} f_{qn}^i f_{p(-n)}^j \quad (26)$$

$$R_{ij}^{lr} = \frac{k_l}{\pi^2 k_o} \sum_{n=-\infty}^{\infty} \sum_{m=-\infty}^{\infty} \frac{J_n'(k_l a_l)}{J_n(k_l a_l)} W_{pm}^{lr}(k_o a_l) f_{qn}^i f_{m(-n)}^j \quad (27)$$

$$f_{pn}^1 = \int_0^\pi e^{jn\phi_l} \sin p\phi_l d\phi_l \quad (28)$$

$$f_{pn}^2 = \int_\pi^{2\pi} e^{jn\phi_l} \sin p(\phi_l - \pi) d\phi_l \quad (29)$$

and the elements of the vector  $\alpha_q^l$  and  $\beta_q^l$  are given by

$$\alpha_q^l = - \sum_{p=1}^{\infty} s_p^l \left\{ j^p J_p'(k_o a_l) \delta_{qp} - j^p J_p(k_o a_l) I_{11}^l \right\} \quad (30)$$

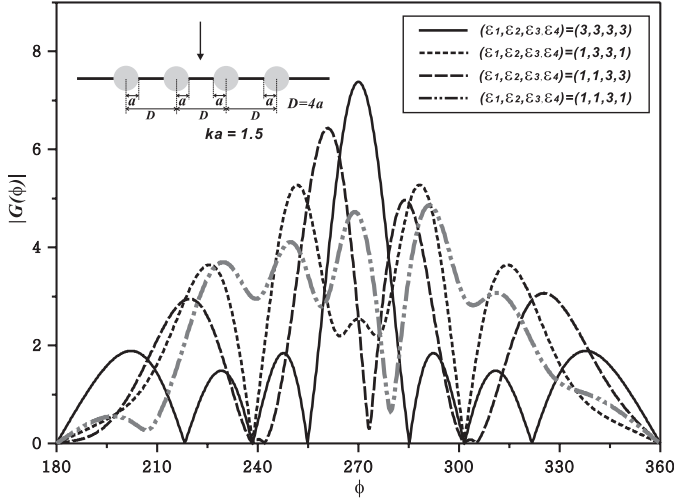


**Figure 10.** Transmitted field pattern ( $|G(\phi)|$ ) from dielectric-loaded four slits with  $ka = 1.5$  at  $\phi_i = 90^\circ$ .

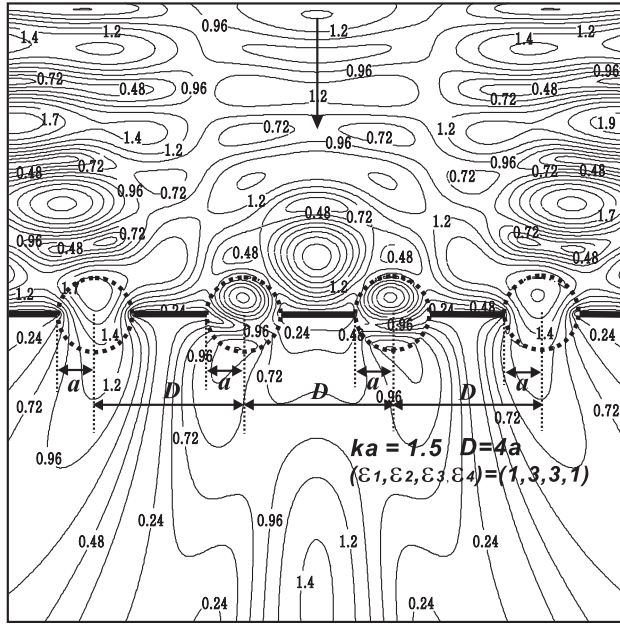


**Figure 11.**  $E$ -field equi-amplitude contour plot near dielectric-loaded four slits with  $ka = 1.5$ ;  $D = 4a$ ,  $(\epsilon_1; \epsilon_2; \epsilon_3; \epsilon_4) = (1; 3; 3; 1)$ .

$$\beta_q^l = \sum_{p=1}^{\infty} s_p^l j^p J_p(k_o a_l) I_{21}^l \quad (31)$$

and the vector  $B_p^l$  and  $C_p^l$  ( $l = 1, 2, 3, \dots, N$ ) represents the unknown expansion coefficients of the scattered and transmitted fields from the dielectric-loaded multiple slits. Eq. (22) can be solved numerically to retrieve the unknown scattering and transmitting coefficients. The transmission field pattern in the far zone ( $k_o \rho \gg 1$  and  $\rho_i > \rho$ ) is determined after using the large argument approximation of the Hankel function and the far-field approximations  $\phi_l \sim \phi$  and  $\rho_l \sim \rho \pm x_l \cos(\phi - \pi)$ , i.e.,

$$E_z^{\text{tran}}(\rho, \phi) = \sqrt{\frac{2j}{\pi k_o \rho}} e^{-jk_o \rho} G(\phi) \quad (32)$$

where

$$G(\phi) = \sum_{r=1}^N \sum_{p=1}^{\infty} j^p C_p^r e^{jk_o x_r \cos(\phi - \pi)} \sin p(\phi - \pi) \quad (33)$$

### 3. NUMERICAL RESULTS

In order to verify that the infinite series involved in the solution is rapidly convergent [21], a far-zone transmitted field of two identical slits is considered. Fig. 2 shows the variation of the far-zone transmitted field for two identical slits ( $k_0 R_1 = k_0 R_2 = 10$ ,  $D = 4k_0 R_1$ ) with the number of the infinite series number of  $p$ ,  $q$ ,  $n$  and  $m$ . As one can see from Fig. 2, the convergence is achieved after  $p = q = n = m = 15$  for a dimension of  $k_0 R_1 = k_0 R_2 = 10$ . That is relatively a small number of terms required to achieve convergence. One of the advantages of the proposed method is the possibility of computing the transmitted field pattern from two slits including or without the mutual interactions by simple setting the elements in the off-diagonal submatrices to zero. To illustrate the effect of mutual interaction of the transmitted field pattern, Figs. 3–6 show the far-transmitted field pattern ( $G(\phi)$ ) of two, three, four and six identical slits with  $ka = 0.5, 1.0, 1.5, 2.0$  at  $\phi_i = 90^\circ$ . The solid and dashed lines represent the patterns with and without mutual interactions (i.e., total and non-interaction fields) between the multiple slits, respectively. The dot-dashed lines represent the patterns of interaction field, which are subtracted from total fields to yield the non-interaction fields. Figs. 7 and 8 show the far-transmitted field pattern at  $\phi = 270^\circ$  of two or four dielectric-loaded slits with  $\epsilon_{1,2,3,4} = 1, 3, 5$  versus  $ka$  in normal incidence. It has been verified that even a slight change in the dielectric-loaded slit can alter the transmitted behavior of multiple slits in a conducting plane. Figs. 9 and 10 show the far-transmitted field pattern of different dielectric-loaded three or four slits. In Fig. 11, the behavior of  $|E_z(\rho, \phi)|$  in the neighborhood of dielectric-loaded four slits ( $\epsilon_1 = 1$ ,  $\epsilon_2 = 3$ ,  $\epsilon_3 = 3$ ,  $\epsilon_4 = 1$ ) is plotted for  $\phi_i = 90^\circ$ . From Fig. 11, it can be seen that the boundary conditions on the conducting plane and dielectric cylinder are satisfied.

### 4. CONCLUSION

The analysis of plane wave scattering and transmitting from dielectric-loaded multiple slits is derived rigorously for TM polarization. The analysis is cast into a form that is simple for computations as well as for predicting the effect of mutual interactions between dielectric-loaded multiple slits.

## REFERENCES

1. Fang, X., M. Cao, Y. Zhou, Y. Ben, and S. Qin, "Fine structure in fresnel diffraction patterns and its application in optical measurement," *Opt. Laser Technol.*, Vol. 29, 383–387, 1997.
2. Smid, P. and P. Horvath, "Fresnel diffraction at an opaque strip expressed by means of asymptotic representations of fresnel integrals," *J. Opt. Soc. Am. A*, Vol. 29, 1071–1077, 2012.
3. Khorshad, A. A., K. Hassani, and M. T. Tavassoly, "Nanometer displacement measurement using Fresnel diffraction," *Opt. Laser Technol.*, Vol. 51, 5066–5072, 2012.
4. Keller, J. B., "Diffraction by an aperture," *J. Appl. Phys.*, Vol. 28, 426–444, 1957.
5. Otsuki, T., "Reexamination of diffraction problem of a slit by a method of fourier-orthogonal functions transformation," *J. Phys. Soc. Jpn.*, Vol. 41, 2046–2051, 1976.
6. Butler, C. M. and D. R. Wilton, "General analysis of narrow strips and slots," *IEEE Trans. Antenna Propagat.*, Vol. 28, 42–48, 1980.
7. Butler, C. M., Y. Rahmat-Sami, and R. Mittra, "Electromagnetic penetration through apertures in conducting surfaces," *IEEE Trans. Antenna Propagat.*, Vol. 35, 82–93, 1987.
8. Kabalan, K. Y., A. El-Hajj, and R. F. Harrington, "Characteristic mode analysis of a slot in a conducting plane separating different media," *IEEE Trans. Antenna Propagat.*, Vol. 38, 476–481, 1990.
9. Yu, J.-W. and N.-H. Myung, "Scattering by a dielectric-loaded nonplanar slit — TM case," *IEEE Trans. Antenna Propagat.*, Vol. 46, 598–600, 1998.
10. Otsuki, T., "Diffraction by two parallel slits in plane," *J. Math. Phys.*, Vol. 19, 911–915, 1978.
11. El-Hajj, A., K. Y. Kabalan, and R. F. Harrington, "Characteristic mode analysis of electromagnetic coupling through multiple slots in a conducting plane," *IEE Proceeding-H.*, Vol. 140, 421–425, 1993.
12. Otsuki, T., "Diffraction by multiple slits," *J. Opt. Soc. Am. A*, Vol. 7, 646–652, 1990.
13. Youn, S. K., H. J. Eom, and J. W. Lee, "Scattering from multiple slits in a thick conducting plane," *Radio Science*, Vol. 30, 1341–1347, 1995.
14. Sun, J. and D. Zeng, "Electromagnetic scattering and absorption by arrays of lossless/lossy metallic or dielectric strips," *Journal of Electromagnetic Waves and Applications*, Vol. 19, No. 4, 497–512,

- 2005.
15. Arnold, M. D., "An efficient solution for scattering by a perfectly conducting strip grating," *Journal of Electromagnetic Waves and Applications*, Vol. 20, No. 7, 891–900, 2006.
  16. Kalhor, H. A. and M. R. Zunoubi, "Modeling optical transmission spectra of periodic narrow slit arrays in thick metal films and their correlation with those of individual slits," *Journal of Electromagnetic Waves and Applications*, Vol. 55, No. 10, 1639–1647, 2008.
  17. Ghazi, G. and M. Shahabadi, "Modal analysis of extraordinary transmission through an array of subwavelength slits," *Progress In Electromagnetics Research*, Vol. 79, 59–74, 2008.
  18. Fu, Y., K. Li, and F. M. Kong, "Analysis of the optical transmission through the metal plate with slit array," *Progress In Electromagnetics Research*, Vol. 82, 109–125, 2008.
  19. Muhn, S. J. and W. S. Park, "Electromagnetic transmission through periodic narrow slit with a finite thickness," *Journal of Electromagnetic Waves and Applications*, Vol. 25, Nos. 14–15, 1930–1939, 2012.
  20. Balaji, U. and R. Vahldieck, "Radial mode matching analysis of ridged circular waveguides," *IEEE Trans. Microwave Theory and Tech.*, Vol. 44, 1183–1186, 1996.
  21. Balanis, C. A., *Advanced Engineering Electromagnetics*, Wiley, 1989.
  22. Stratton, J. A., *Electromagnetic Theory*, IEEE Press, Wiley, 2007.